

Accuracy of Image Transforms in Feature Extraction for Multimodal Biometric Systems

Sanyamee Patel, Aarvi A Thadeshwar, Dhruvi Patel, Ratnesh Chaturvedi

Abstract—With an increased need for security in organisations around the world, it becomes necessary to have in place a system that is mostly foolproof, in order to prevent duping and unauthorised access to sensitive information. Each individual can be distinguished from another with biometric attributes, like the face, fingerprint and iris scan. There exist two kinds of systems that employ varying numbers of these traits for verification and recognition—unimodal and multimodal. Unimodal systems employ one trait, hence allowing easy misuse and duping. Multimodal systems, however, employ two or more of these traits. They allow access to a person only if they show a match all of the traits that exist for them in the database. In our project, we carried out fusion of four attributes—face, fingerprint, knuckle print and iris scan, in order to exhibit verification. We applied different transforms to the attributes and compared the results.

Index Terms— Unimodal Biometrics, Multimodal Biometrics, Image Transforms, Pre-processing, Verification.

1 INTRODUCTION

A biometric is a technical term that encapsulates body measurements and calculations. It describes human characteristics that may be used to differentiate one person from another. Hence, biometric authentication is the form of authentication and access control, wherein an individual is verified for legitimacy against a set of recognisable and verifiable data which is unique and specific to them.[1] The process involves comparing the testing data to a stored biometric template in order to determine resemblance.

The demand for biometrics is rising quickly due to an increased need for security in every organisation of the world. Sensitive data and equipment require reliable security systems, the demand of which is fulfilled by biometric systems to regulate access[2]. All such systems employ several existing techniques for unimodal biometrics.

A unimodal biometric system uses a single biometric such as a fingerprint or an iris scan to recognize an individual[3]. However, these systems can be compromised with little difficulty, putting the privacy and security of an organization or an individual at stake[4]. The increase in duping gives rise to a requirement for constructing an efficient system using multiple biometric attributes.

A system employing multiple biometric attributes to verify the identity of an individual is a multimodal biometric system. In multimodal systems, an initial image correction measures readies the images for further processing by reducing noisy elements that may hamper the performance of the system. Various image transforms are then applied to derive the feature vectors of the attributes. This leads to reduced image size, since the transforms eliminate unnecessary information. Biometric recognition is a system which recognizes an individual based on some features derived from behavioral or physiological characteristics. Feature extraction is used to represent important parts of an image in the form of a feature vector. This approach is useful when image sizes are large and

a reduced feature representation is required to quickly complete tasks such as image matching and retrieval. [5] Transformation of input data into a set of features is carried out. Features are distinctive properties of input patterns that help in differentiating between the categories of input pattern. Most of the real-life biometric systems are unimodal biometric recognition, which are based on single traits of biometric information. Such systems are affected by many problems like noise, non-universality, duping and unacceptable error rates etc. Hence multimodal biometric identification systems are becoming popular in these days. [6]

Our project involved an initial review of existing multimodal systems, which allowed us to understand the various techniques used in combining different combinations of biometrics. We then decided upon some of the most prevalent attributes that are used to identify a person—the iris[7], the fingerprint, and the face. We added the attribute of the knuckle print to test how a rarely used trait would elevate the efficiency of the system.

Once we performed pre-processing on individual images, they were made to undergo transforms that allowed us to reduce the size of the image. We further stitched all four attributes to form another $n \times n$ image. These made up the training data for the system. A testing image was made to undergo the same pre-processing and transform stages, and then compared to the training data using distance measures for image comparison. The results that various transforms gave were noted and contrasts were made to determine the most efficient ones in terms of Genuine Acceptance Rate and False Acceptance Rate.

2 PROPOSED ARCHITECTURE

The proposed system is software-centric. The images used for training and testing have been acquired from online sources. The databases consist of eight images each for an individual. Of these, seven are used for training purposes, and one is used for testing.

Since the images have been acquired beforehand, the hardware details are drawn for representation purposes. The software architecture consists of the different techniques required for pre-processing the images. These include illumination correction, noise removal, and reduction of unnecessary information (Figure 1). The attributes are then made to undergo different transforms individually, and then stitched together to form the training data for the persons first image of each attribute. The data is to be stored in the form of .mat files.

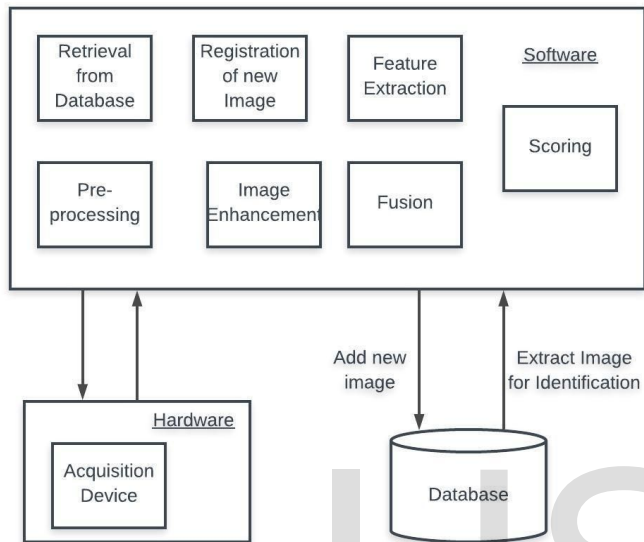


Figure 1. Proposed Architecture

3 PROPOSED ALGORITHM

The following steps summarize the entire process of the proposed multimodal biometric system (Figure 2):

1. Pre-processing of biometric images
 - a. Finger: Binarization using global thresholding
 - b. Iris: Canny edge detection and circular Hough transform
 - c. Face: Convert to grayscale
 - d. Knuckle: Canny edge detection
2. Feature vector extraction using all transforms and stitching LL bands together for each biometric
3. Matching of feature vector using Euclidean distance and Manhattan distance for each transform system.
4. GAR and FAR calculated for each transform system by sorting the array obtained for Manhattan and Euclidean distance.

4 DATABASE DESIGN

The database consists of scans of the fingerprint, knuckle print, iris and face. For ten individuals, there exist eight images each, of which seven are used for training, and one for testing. Each image is in .bmp/ .jpg format, which is first stored as .mat files for easy operation. The fingerprint images are $n \times n$. However, those of the face, knuckle and iris are $p \times q$, and are resized to square images by padding zeros. Every

individual is recognised using a unique id allocated in the range 70021014060 and 70021014069. Sources for each biometric database are as follows:

- Face- Yale Face Database
- Iris- IIT Delhi Iris Database (Version 1.0)
- Finger- CASIA Fingerprint Image Database Version 5.0
- Knuckle- IIT Delhi Finger Knuckle Database (Version 1.0)

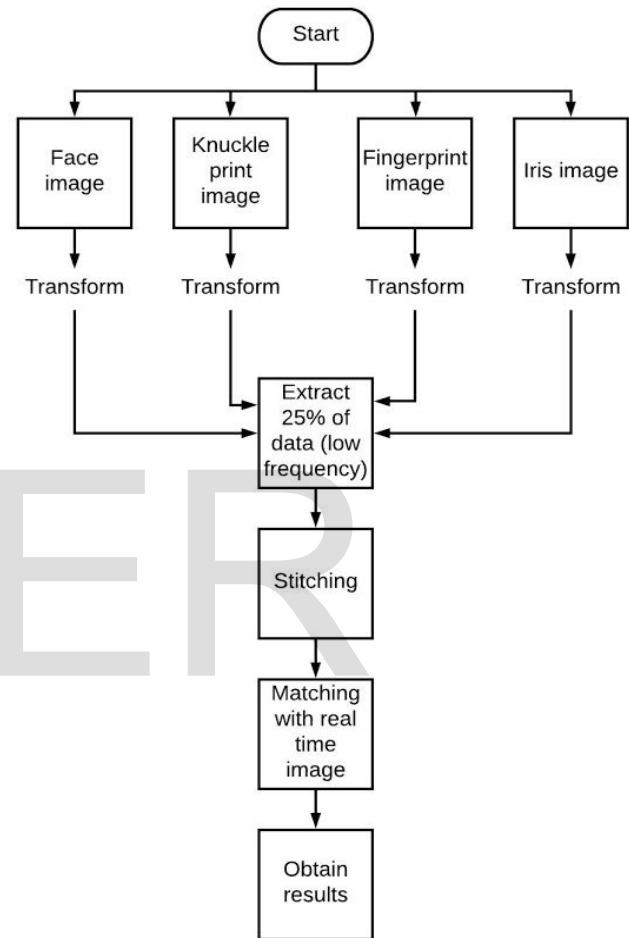


Figure 2. Proposed Algorithm

5 PRE-PROCESSING

The padded images were further resized such that their dimensions were in the order of 2. The dimensions being in this scale are important for accurate processing of transforms.

Each attribute was then resized and then pre-processed using a technique suitable for each. The following methods were used to make images appropriate for processing.

5.1 Knuckle

The knuckle print was processed using two functions and results were compared. Canny edge detector and Gaussian smoothing filter (Figure 3) were applied to different copies of the same image. The degree of smoothing was first varied.

Further, canny edge detector was applied on the smoothed images (Figure 4). A separate operation of only using canny edge detector was also performed. [8]

It was observed that the smoothing operations led to quite a large amount of information loss. This was the basis of selection of only the canny edge detector. Hence, this technique allowed the output images to have more prominent edges and a sufficient amount of information.

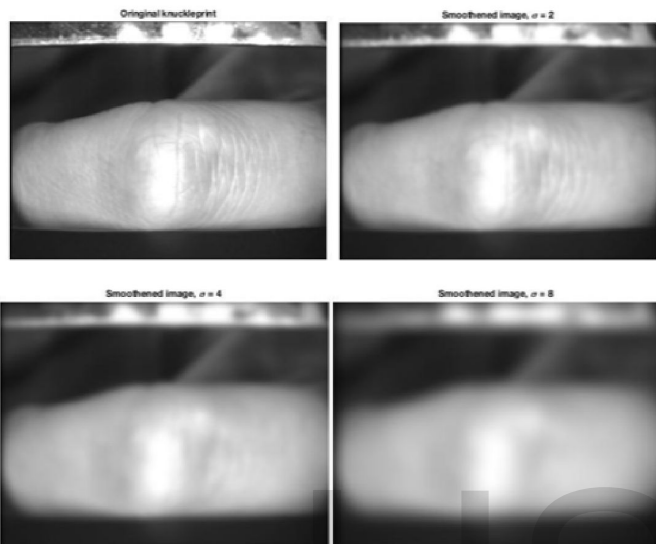


Figure 3. Smoothing operation on knuckle print

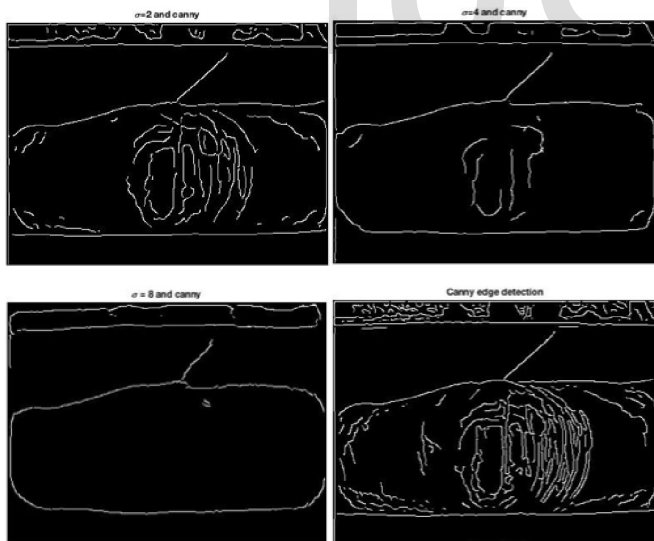


Figure 4. Smoothing followed by canny edge detection on knuckle print

2.2 Fingerprint

The fingerprint images were in the form of RGB (Red-Green-Blue) planes. They were first converted to grayscale images. Roberts cross operator and binarization using global thresholding were applied to different copies of the same image to compare results. Results of both operations

is shown in Figure 5. [9]

It is evident that Roberts cross operator causes loss of information while thresholding using binarization yields an image with more prominent edges, and sufficient information as required. Hence, the pre-processing of fingerprint image is carried out by binarization using global thresholding.

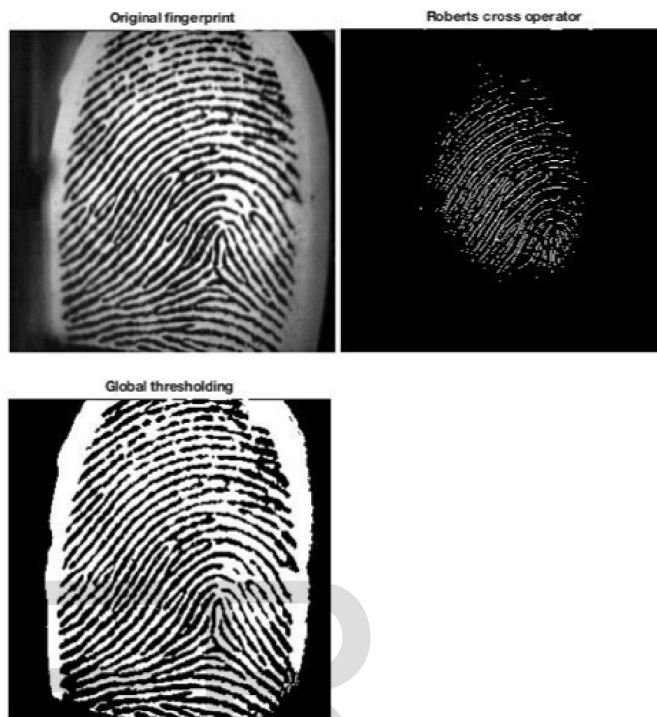


Figure 5. Comparison of pre-processing for fingerprint

2.3 Face

The images of the face in the RGB plane were converted from 24 bit image to 8 bit image. The acquired images needed to be padded with zeros in order to make the image size appropriate for transformation.[10] They were then resized to 256 x 256.

2.4 Iris

Pre-processing of iris image requires identification of region of interest, i.e. the circular region consisting of the iris. This is done by application of Canny edge detector (Figure 6) and Circular Hough Transform on the image. The canny edge detector detects the circle approximately on the original image.

Circular Hough transform is then applied on the processed image to mark the points of the circle. [11]

Elimination of area outside ROI is done by creating a mask using the circle coordinates or simply by coloring the pixels outside the circle blue. The second solution is used in the final system as the resulting image after application of the mask had errors and gives only an approximate position of ROI (Region of Interest) (Figure 7).

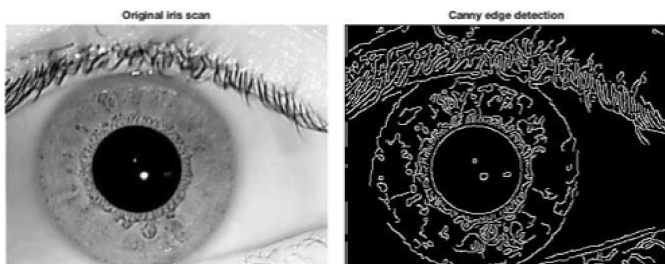


Figure 6. Edge Detection of Iris

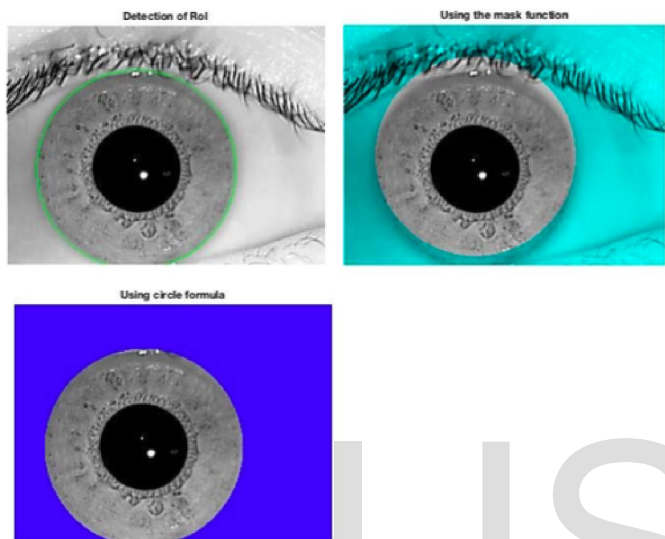


Figure 7. Region of interest for Iris

6 FEATURE EXTRACTION

Feature vector in the proposed system is extracted by applying one image transform to the pre-processed images. The following seven transforms are applied to all biometrics for comparison in order to determine the transform for optimum results.

- Discrete Sine Transform
- Discrete Cosine Transform
- Haar Transform
- Kekre Transform
- Slant Transform
- Hartley Transform
- Walsh Transform

The parts of the transformed image which have the maximum information are selected for each biometric. These images of iris, finger, knuckle and face are stitched into LL, LH, HL and HH bands respectively. This image is then saved in a .mat file format and used as a feature vector for further operation. Feature vectors are developed for all 8 samples present in the database.

7 MATCHING

Out of the eight feature vectors developed for an individual, the first seven are used for training the dataset and the last i.e.

eight image is used for testing. The eighth image of each individual is matched against every image of all individuals. This is done by calculating the Euclidean distance and the Manhattan distance between the test and training images.

8 SCORING

Genuine Acceptance Rate (GAR) and False Acceptance Rate (FAR) are the two parameters used to measure the robustness of the system. [12]. They are calculated for each transform system according to the number of entries it accepts correctly and rejects incorrectly. They are calculated using the following equations.

$$GAR = \frac{\text{Number of Correct Acceptance}}{\text{Number of Identification Attempts}} \quad (1)$$

$$FAR = \frac{\text{Number of False Acceptance}}{\text{Number of Identification Attempts}} \quad (2)$$

9 RESULTS AND DISCUSSION

The testing process first involves taking as input from user the identity of the person whose test image is to be supplied to the system. The distance measure calculations of the same are done against every image in the database. The following subsections show the GAR and FAR obtained for feature set of each transform. The number of training images are 7, hence the value is taken as the basis for calculation of the rates. A GAR value of 1 would indicate 100 percent accuracy in matching, while that of 0 indicates failure to match, and vice-versa for the calculated value of FAR.

9.1 Discrete Cosine Transform

DCT is the best performer, since it exhibits 100 percent accuracy for Manhattan distance, and the highest accuracy for Euclidean. (Table I)

Person No.	Image No.	Euclidean Distance	Person No.	Image No.	Manhattan Distance
5	5	9826.616725	5	3	881121.22101
5	7	10792.636277	5	1	887499.52892
5	1	11831.084629	5	5	888591.26860
5	3	12212.445354	5	7	891372.61841
5	2	14501.156808	5	6	961136.80497
2	5	19133.887050	5	4	985707.99988
2	3	19197.468532	5	2	1011486.0669
2	1	20329.766678	3	7	1028435.9859
5	4	20701.278253	2	4	1034484.9490
5	6	21686.297848	2	6	1040489.4168
GAR		0.71	GAR		1
FAR		0.285	FAR		0

Table I. GAR and FAR for DCT

9.2 Haar Transform

Haar transform is the poorest, since the values of GAR and FAR are highly undesirable. (Table II)

Person No.	Image No.	Euclidean Distance	Person No.	Image No.	Manhattan Distance
4	7	23969.771959	3	7	673718.67098
3	7	25305.518869	2	6	740117.92228
7	6	27077.522289	5	6	744746.84323
5	6	27428.808446	3	4	761775.06671
7	4	28397.074347	4	4	764846.14066
3	4	29488.078798	4	7	765655.08386
1	6	30632.566722	2	4	770284.90944
6	7	30997.068176	5	4	772037.02316
6	5	31400.208543	3	1	776979.26025
6	2	31514.490512	6	1	786313.21095
GAR		0.14	GAR		0.14
FAR		0.85	FAR		0.85

Table II. GAR and FAR for Haar Transform

9.3 Hartley Transform

Hartley transform is one of the most accurate, since it gives good accuracy for Manhattan and Euclidean distances. (Table III)

Person No.	Image No.	Euclidean Distance	Person No.	Image No.	Manhattan Distance
5	1	20508.481752	5	1	852831.93987
5	7	20534.272644	5	3	858437.82895
5	5	20710.705913	5	5	865473.59906
5	3	20844.294994	5	2	867370.78024
5	2	21540.536542	5	7	873321.19209
2	5	21828.930016	5	4	873770.40487
2	1	21864.541111	2	5	875178.54910
9	2	21978.551635	4	4	876204.16930
9	5	22165.757119	9	2	880906.90971
5	4	22268.267664	3	1	881219.07316
GAR		0.71	GAR		0.85
FAR		0.285	FAR		0.14

Table III. GAR and FAR for Hartley Transform

9.4 Kekre Transform

Kekre transform performs poorly for both distance calculations. (Table IV)

Person No.	Image No.	Euclidean Distance	Person No.	Image No.	Manhattan Distance
5	6	110864889.05	5	6	12212478851
4	7	122668663.17	4	7	13083617876
3	7	125752555.22	3	7	14504675378
7	6	144682047.25	5	4	15533825320
10	6	153784884.60	7	6	16187963287
1	6	156126383.77	4	6	16527389541
5	4	169089937.97	5	2	17119385022
9	6	169834696.21	5	1	17251970610
5	1	175074265.84	1	6	17302707806
4	6	178930717.92	9	6	17574462405
GAR		0.285	GAR		0.42
FAR		0.71	FAR		0.57

Table IV. GAR and FAR for Kekre Transform

9.5 Slant Transform

The slant transform is among the least accurate, due to the small values of GAR, and large values of FAR. (Table V)

Person No.	Image No.	Euclidean Distance	Person No.	Image No.	Manhattan Distance
6	1	30422.030147	5	4	1107035.9760
5	4	30700.522631	4	7	1112677.5366
5	1	30938.716549	3	7	1115326.4526
1	3	31283.993668	5	6	1116921.2961
1	1	31669.834774	4	4	1118821.5659
4	4	31763.600021	3	4	1120897.2107
6	4	31767.526998	2	4	1126864.5895
9	6	31926.060609	6	1	1132885.8397
4	1	31998.248680	2	6	1145376.7367
2	4	32361.571682	1	6	1146613.8895
GAR		0.28	GAR		0.28
FAR		0.71	FAR		0.71

Table V. GAR and FAR for Slant Transform

9.6 Walsh Transform

Walsh transform, like Hartley, is one of the most accurate, since it gives good accuracy for Manhattan and Euclidean distance. (Table VI)

Person No.	Image No.	Euclidean Distance	Person No.	Image No.	Manhattan Distance
5	5	15282.370666	5	6	1107309.2610
5	3	16381.978416	5	3	1109733.7250
5	7	16412.595499	5	4	1116358.6782
5	1	16937.819279	5	5	1122840.4564
5	2	17748.613842	5	1	1137045.9759
2	3	20525.260184	3	7	1163207.1076
2	5	21629.777930	5	7	1170178.1000
2	1	22420.300123	4	7	1177478.5327
5	4	22548.932446	2	6	1181050.8336
9	1	22621.756604	5	2	1182671.6060
GAR		0.71	GAR		0.85
FAR		0.28	FAR		0.14

Table VI. GAR and FAR for Walsh Transform

9.7 Discrete Sine Transform

DST exhibits accuracy only when the Euclidean distance is used as a measure for comparison, hence it is not completely accurate on comparison with other transforms. (Table VII)

Person No.	Image No.	Euclidean Distance	Person No.	Image No.	Manhattan Distance
6	1	25570.676015	3	7	1134711.7740
8	2	26896.342445	3	4	1163177.3509
5	1	27149.213205	5	6	1181635.6326
5	5	27406.432032	4	7	1197713.4738
5	3	27607.877887	2	6	1234196.8970
5	4	27668.888522	1	6	1240431.6449
3	3	27785.932599	2	4	1255792.4127
4	6	27833.014382	3	2	1258914.8429
3	2	27924.716137	6	1	1260086.0730
4	4	27945.835592	5	4	1260926.6464
GAR		0.57	GAR		0.14
FAR		0.42	FAR		0.85

Table VII. GAR and FAR for DST

9.7 Visual Representation of Accuracy Comparison

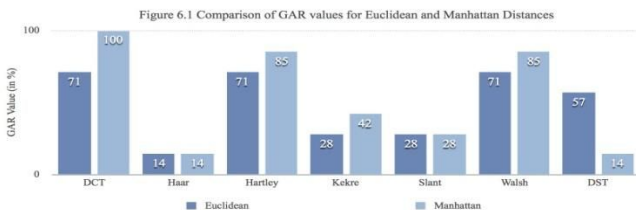


Figure 8. Comparison of GAR for various transforms

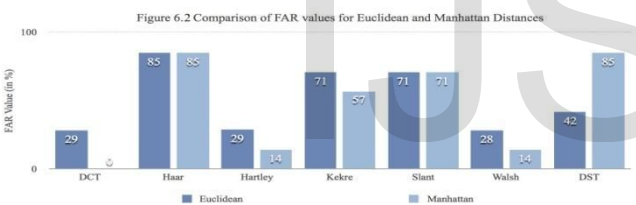


Figure 9. Comparison of FAR for various transforms

10 CONCLUSION AND FUTURE SCOPE

Biometrics is an emerging field due to the increased need for security. Unimodal biometrics comes with the disadvantage of illegal penetration by unauthorised personnel. This is overcome by using multiple biometric attributes for the purpose of authentication.

Our research project proposes a fusion approach incorporating the second level decomposition of images. Each biometric will be decomposed and the LL bands extracted. Further, each LL band will be substituted for the other three bands in one of the biometric decompositions to produce a single image containing fused information. This can undergo inverse transforms to give a feature extracted fused image as output. As observed, DCT, Walsh and Hartley are the most efficient transforms when considering the distance measures of Manhattan and Euclidean. DCT is efficient, since most of the information is concentrated in the

upper left corner of the transformed image. Hartley transformed images contain information in the corners of the image, which we have efficiently extracted. Our system hence is mostly efficient for these transforms, as observed in Figures 8 and 9. In the future, we would like to add Eigenface extraction for face, such that the storage required for the same is reduced even further. We aim to also improve the efficiency of the other transforms.

REFERENCES

- [1] A. K. Jain, A. Ross, and S. Pankanti, "Biometrics: A tool for information security," *IEEE Trans. Inf. Forensics Security*, vol. 1, no. 2, pp. 125–143, Jun. 2006.
- [2] E. Zureik and K. Hindle, "Governance, security and technology: The case of biometrics," *Stud. Political Econ.*, vol. 73, no. 1, pp. 113–137, 2004.
- [3] S. Latifi and N. Solayappan, "A survey of unimodal biometric methods," in *Proc. Int. Conf. Secur. Manage.*, 2006, pp. 57–63.
- [4] S. M. S. Ahmad, B. M. Ali, and W. A. W. Adnan, "Technical issues and challenges of biometric applications as access control tools of information security," *Int. J. Innov. Comput. Inf. Control*, vol. 8, no. 11, pp. 7983–7999, Nov. 2012.
- [5] K. Tewari and R. L. Kalakoti, "Fingerprint recognition and feature extraction using transform domain techniques," in *Proc. Int. Conf. Adv. Commun. Comput. Technol. (ICACACT)*, Aug. 2014, pp. 1–5.
- [6] Oloyede, Muhtahir O., and Gerhard P. Hancke. "Unimodal and multimodal biometric sensing systems: a review." *IEEE Access* 4 (2016): 7532-7555.
- [7] S. R. Ganorkar and A. A. Ghatol, "Iris recognition: An emerging biometric technology," in *Proc. 6th WSEAS Int. Conf. Signal Process., Robot. Autom.*, Feb. 2007, pp. 91–96.
- [8] Meraoumia, Abdallah, Salim Chitroub, and Ahmed Bouridane. "Robust multimodal biometric identification system using Finger-Knuckle-Print features." In *Control, Engineering Information Technology (CEIT), 2015 3rd International Conference on*, pp. 1-6. IEEE, 2015.
- [9] P. Pakutharivu and M. Srinath, "A comprehensive survey on fingerprint recognition systems," *Indian J. Sci. Technol.*, vol. 8, no. 35, pp. 1–7, Dec. 2015.
- [10] Jain, Anil K., Lin Hong, and Yatin Kulkarni. "A multimodal biometric system using fingerprint, face and speech." In *Proceedings of 2nd Int'l Conference on Audio-and Video-based Biometric Person Authentication*, Washington DC, pp. 182-187. 1999.
- [11] Aizi, Kamel, Mohamed Ouslim, and Ahmed Sabri. "Remote multimodal biometric identification based on the fusion of the iris and the fingerprint." In *Electrical Engineering (ICEE), 2015 4th International Conference on*, pp. 1-6. IEEE, 2015.
- [12] ARAVALLI, NAGAMMA. "Automatic System for Person Authentication by Multimodal Biometrics- A Survey."